Macromolecules

pubs.acs.org/Macromolecules Article

Chemomechanics Underpinning the Growth and Strengthening Behaviors of Mechanoresponsive Self-Growing Hydrogels

Zhi Sheng, Jie Ma, Zihang Shen, Shaoxing Qu, and Zheng Jia*

Cite This: https://doi.org/10.1021/acs.macromol.3c00837 Read Online

ACCESS | Metrics & More | Article Recommendations | Supporting Information

ABSTRACT: Living tissues, such as skeletal muscles, are capable of remodeling and self-growth in response to their mechanical environment. In contrast, synthetic materials, once formed, have little ability to grow and reconstruct. Recently, mechanoresponsive self-growing hydrogel, a novel hydrogel that can grow under mechanical stresses, has been reported. However, the chemomechanics underpinning the growth and strengthening behaviors of mechanoresponsive self-growing hydrogels remains largely unexplored. Here, we present a chemomechanical model for mechanoresponsive self-growing hydrogels by developing and integrating theories of mechanoradical generation due to chain rupture, chemical kinetics of polymerization, and new network formation. The chemomechanical model is applied to theoretically investigate the concentration of mechanoradical generated by stretching hydrogels, the polymerization kinetics of monomers and cross-linkers, and the strengthened mechanical behavior of self-growing hydrogels due to new network formation. Finally, we employ the theory to predict the stress−stretch responses of self-growing hydrogels under repetitive loading−unloading and growth cycles in the closed system. The results, especially the predicted ultimate stresses of the hydrogel over cycles, agree well with experimental measurements made by Matsuda et al. and can consistently explain the experimentally observed mechanical behaviors of self-growing hydrogels.

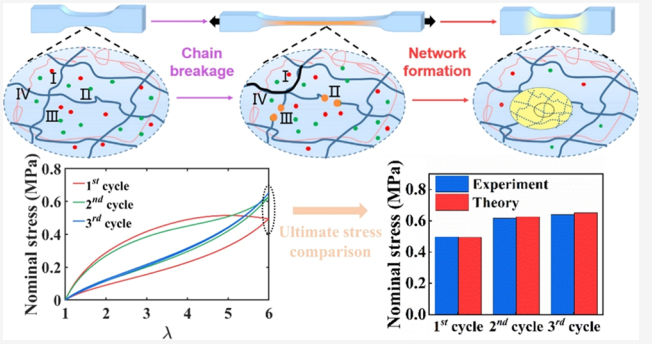

1. INTRODUCTION

Since the advent of synthetic hydrogels, they have attracted much attention for their wide range of applications, including but not limited to drug delivery systems,[1,2] tissue engineering,[3,4] flexible electronics,[5,6] supercapacitors,[7] etc. High water content endows hydrogels with advantages such as biocompatibility and optical transparency but also leads to the brittle mechanical behavior of hydrogels by diluting the polymer chains that transmit mechanical forces.

To improve the mechanical properties of hydrogels to meet the requirements of practical applications, researchers have proposed various methods to engineer the network structure of hydrogels. For example, the toughness and strength of hydrogels can be greatly improved by introducing strain-induced crystallization,[8] dense entanglements,[9] and force-triggered chemical reactions[10] into hydrogels. As opposed to synthesizing hydrogels of a single network, designing double-network (DN) hydrogels has become a mainstream approach to toughen and strengthen hydrogels in the past two decades. DN hydrogels were first synthesized by Gong and co-workers,[11] which consist of two distinct networks: a brittle short-chain network that breaks sacrificially upon stretching to dissipate large amounts of energy and a stretchable long-chain network that maintains the elasticity of the hydrogel.[12] The first synthetic DN hydrogels are fully cross-linked by chemical cross-linkers and thus suffer from irreversible network damage, poor fatigue resistance, and severe softening.[13] To address the issue, researchers introduce a physically cross-linked network, which is based on ionic bonds,[14] coordination interactions,[15] hydrogen bonds,[16] hydrophobic associations,[17] etc., as the sacrificial short-chain network of DN hydrogels. This type of network toughens the gel through a continuous energy dissipation mechanism and imparts self-healing properties to the DN hydrogel.[18,19] Along this line, fully physically cross-linked DN hydrogels[20] are also synthesized, attaining even better self-healing ability.

Many of the DN hydrogels described above can fully or partially restore their mechanical strength after deformation; however, they cannot remodel their network structure to improve their mechanical properties, in contrast to living tissues, which can strengthen themselves by growing and remodeling to adapt to their surrounding mechanical environ-

Received: April 30, 2023
Revised: August 9, 2023
Accepted: November 6, 2023

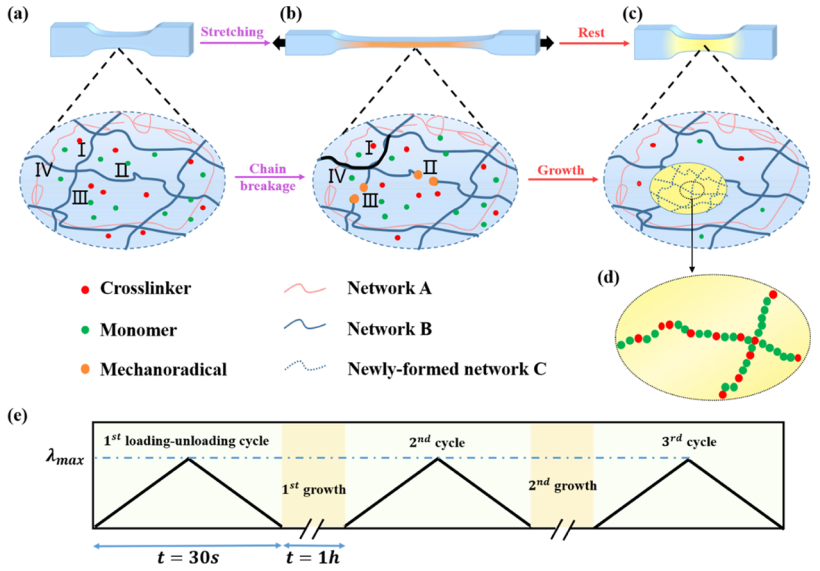

Figure 1. Schematics of the growth process of self-growing hydrogels. (a) Original DN hydrogel with intact double networks. (b) Chain breakage and mechanoradical generation due to hydrogel deformation. (c) Formation of a new network due to mechanoradical-triggered polymerization of monomers and cross-linkers supplied from external environment. (d) Zoomed-in view showing the network composition of the newly formed network. (e) Time profiles of the repetitive stretching and incubation of self-growing hydrogels.

ment. Recently, Matsuda et al.[21] proposed a novel strategy to strengthen DN hydrogels by designing mechanoresponsive self-growing hydrogels inspired by muscle training. It is well known that muscles become larger and stronger through repeated exercise when provided with sufficient nutrients (e.g., amino acids). DN hydrogels can be strengthened by using a similar mechanism: mechanical stress breaks the brittle short-chain network of DN hydrogels during the stretching of hydrogels and ruptures covalent bonds of the polymer chains, generating a sufficiently high concentration of mechanoradicals at the broken ends of the brittle network strands.[21−23] These mechanoradicals can trigger the polymerization of monomers and cross-linkers supplied from the external environment to form additional new networks, thus strengthening the hydrogel. Self-growing DN hydrogels can heal and even strengthen under repeated mechanical stress, paving the way for the development of soft robots and smart devices that can adapt to the demanding mechanical environment.

Many theoretical models have been developed to study the mechanics of various emerging hydrogels, including self-healing hydrogels,[24−27] nanocomposite hydrogels,[28,29] photosynthesis-assisted polymer,[30] hydrogels with dynamic metal-coordinated bonds,[31] etc. For DN hydrogels, various aspects of mechanical behavior have been theoretically investigated, including damage under large deformation,[32,33] viscoelasticity,[34,35] multiaxial deformation,[36] delayed necking instability,[37] swelling behaviors,[38] and fracture processes.[39,40] Nevertheless, most existing theories of growth focus on the growth of biological tissues. For instance, Jia and Nguyen[41] investigated the growth and remodeling of collagenous tissues based on concurrent collagen deposition and degradation. Liu et al.[42] presented a mechanical model to study the influence of geometric incompatibility on pattern selection of growing bilayer soft tubes. Even fewer mechanical models have been developed for the growth of hydrogels. Fan and Chen[43] developed a micromechanical model to study the growth of hydrogel networks, but the chemical kinetics of growth was not taken into account. Recently, Zhang and Hu[44] nicely proposed a comprehensive statistical-chain-based theoretical framework for dynamic living polymeric gels, where they discussed various chain remodeling reactions of the gels, including the formation of new chains (i.e., gel growth). However, the model ignores some key microscopic features of self-growing hydrogels at the molecular scale (e.g., force-induced generation of mechanoradicals, network structure and composition of newly formed network, and the self-strengthening mechanical behavior) such that a chemomechanical model of mechanoresponsive self-growing hydrogels is still lacking.

The aim of this work is to develop a chemomechanical model capable of explaining various mechanical phenomena of self-growing hydrogels, in particular, self-growth and strengthening. We first formulate a quantitative expression for the force-induced generation of mechanoradicals by extending the network alteration model.[33,45] Then, we introduce the chemical kinetics of mechanoradicals to simulate the polymerization process of supplied monomers and cross-linkers during self-growth, which predicts the network structure and composition of newly formed networks. Finally, the self-strengthening behavior of mechanoresponsive self-growing hydrogels after growth is studied based on the interpenetrating network model.[33] The results are compared with experimental measurements of Matsuda et al.[21] to validate the chemomechanical model, and some important experimental observations can be consistently explained by the model. The plan of the paper is as follows. Section 2 reports the chemomechanical model of the self-growing hydrogels, which quantitatively incorporates the process of mechanoradical generation, the chemical kinetics of new network polymerization, and the mechanical behavior of self-growing hydrogels after the formation of new networks. Section 3 discusses the effects of mechanoradical concentration, polymerization reaction rates, and initial concentrations of supplied monomers and cross-linkers on self-growth. In Section 4, we theoretically predict stress−stretch responses of self-growing hydrogels under repeated loading−unloading cycles and compare the results

https://doi.org/10.1021/acs.macromol.3c00837
Macromolecules XXXX, XXX, XXX−XXX

to experimental measurements. Conclusions are listed in Section 5.

2. THEORETICAL MODEL

In this section, we develop a chemomechanical model for mechanoresponsive self-growing hydrogels. The model aims to theoretically explain the growth and strengthening of self-growing hydrogels under repeated mechanical stresses observed in the experiments of Matsuda et al.,[21] in which hydrogel samples are cyclically stretched with a 1 h growth period between every two consecutive loading−unloading cycles (Figure 1). The model quantitatively takes into account a number of key features of the gel growth process, including mechanoradical generation induced by chain rupture, chemical kinetics of the polymerization of new networks, and the strengthened mechanical behavior of self-growing hydrogels after growth. To focus on essential ideas, we study self-growing hydrogels prefed with a monomer/cross-linker solution—which is referred to as a closed system by Matsuda et al.[21]—so that the hydrogel does not exchange substance with surroundings, and its overall volume remains constant during deformation and growth. To this end, in the following, the undeformed self-growing hydrogel is taken as the reference state to formulate the theory.

2.1. Chain-Rupture-Induced Mechanoradical Generation. The original self-growing hydrogel is a DN hydrogel that contains a stretchable long-chain network A and a brittle short-chain network B. To describe the network structure of the self-growing hydrogel, we let N_i be the number of the ith chain per unit volume of the ith network (i.e., chain density) and n_i be the number of freely jointed links of the ith chain (i.e., chain length), where i = A or B for a DN hydrogel. Upon stretching, the long polymer chains in network A remain intact and maintain the elasticity of the hydrogel, while the chains in network B break sequentially. Figures 1a and 1b illustrate the physical picture. Consider four chains I, II, III, and IV in network B. When the hydrogel is deformed, some chains such as chains II and III break and become inactive dangling chains that do not contribute to the elasticity of the network; as a result, the intact chains I and IV rearrange into one longer chain (i.e., chain I plus chain IV) with higher number of links. That is, there are originally four short chains, but only one long chain remains after mechanical loading. The chains' breakage (e.g., chain b and c) and rearrangement (e.g., chain a and d) collectively lead to a decrease in average chain density and an increase in the average chain length of network B. The above damage process can be quantitatively described by the network alteration model,[33,45] i.e.,

$$N_B = N_{B0}\exp[-p_B(\Lambda_B^{max} - C_B^{-1/3})] \tag{1a}$$

$$n_B = n_{B0}\exp[q_B(\Lambda_B^{max} - C_B^{-1/3})] \tag{1b}$$

where N_B and n_B are the current chain density and chain length, N_{B0} and n_{B0} are the initial chain density and chain length in network B, Λ_B^{max} is the maximum stretch of the chains in network B in the loading history, C_B is the volume fraction of network B in the self-growing hydrogel, and p_B and q_B are the damage parameters that characterize the decrease of chain density and increase of chain length of the network B, respectively.

As shown in Figure 1b, chain breakage of network B not only results in changes in chain density and chain length but also generates mechanoradicals at both ends of the broken chain—one broken polymer chain can produce two mechanoradicals,[21] just like one photoinitiator decomposing into two free radicals.[46,47] Therefore, in order to assess the number of mechanoradicals generated, one needs to calculate the number of chains ruptured due to stretching of the hydrogel. Note that the initial chain density per unit volume of the hydrogel and the chain length of network B are C_BN_{B0} and n_{B0}, respectively, such that the number of links per unit volume of the hydrogel is originally $C_BN_{B0}n_{B0}$. During the deformation of the hydrogel, the chains in network B break and the ruptured chains become inactive dangling chains that no longer contribute to the chain density and chain length. Therefore, the chain density per unit volume of the hydrogel and the chain length of network B become C_BN_B and n_B, resulting in $C_BN_Bn_B$ number of remaining active links per unit volume of the hydrogel. To this end, the total number of links entering inactive dangling chains per unit volume of the hydrogel is

$$c_{ld} = C_BN_{B0}n_{B0} - C_BN_Bn_B \tag{2}$$

These inactive links come from ruptured chains whose initial length is n_{B0}. According to eq 2, the number of broken chains per unit volume of hydrogel can be given by

$$c_{bc} = \frac{c_{ld}}{n_{B0}} = C_BN_{B0} - \frac{C_BN_Bn_B}{n_{B0}} \tag{3}$$

Considering that one ruptured chain generates two mechanoradicals, we can obtain the number of mechanoradicals per unit volume of the hydrogel (i.e., the concentration of mechanoradicals in the gel) as follows

$$c_{ra} = 2c_{bc} \tag{4}$$

Substituting eqs 1a, 1b and 3 into eq 4 and taking into account the volume conservation condition $N_{B0}n_{B0}\nu_B = 1$, we have the concentration of mechanoradicals in the hydrogel as

$$c_{ra} = \frac{2C_B}{\nu_Bn_{B0}}(1 - \exp[(q_B - p_B)(\Lambda_B^{max} - C_B^{-1/3})]) \tag{5}$$

where ν_B is the volume of one link in network B. The network alteration process requires $p_B \geq q_B > 0$,[33] because in this process, the chain density decreases, the chain length increases, and the total number of links in the network needs to satisfy mass conservation condition and thus cannot increase. If $p_B = q_B$, N_Bn_B remains constant (i.e., $N_Bn_B = N_{B0}n_{B0}$) and $c_{ra} = 0$. If $p_B > q_B$, we have $c_{ra} > 0$, which means that mechanoradicals are generated due to chain breakage during hydrogel stretching.

2.2. Chemical Kinetics of the Polymerization of New Networks. Mechanoradicals generated due to chain scission can trigger the polymerization of supplied monomers and cross-linkers, thereby leading to stress-induced formation of new networks.[21] A typical polymerization process consists of some key steps for growing polymer networks, including chain initiation, chain propagation, chain transfer, and chain termination.[46] For the self-growing hydrogels studied in this work, polymerization is initiated by the mechanoradicals after a sufficient amount of them is generated. Upon encountering a monomer, a mechanoradical reacts with the monomer, opening the C═C double bond on the monomer and transferring the free radical to the monomer. The new free radical meets another monomer and repeats the process. This process, termed chain propagation, turns monomers into a

https://doi.org/10.1021/acs.macromol.3c00837
Macromolecules XXXX, XXX, XXX−XXX

growing polymer chain. The propagation process can also incorporate cross-linkers into the growing polymer chain, eventually leading to the formation of a new network, as shown in Figure 1c. Chain transfer has not been reported for self-growing hydrogels[21] and is thus not considered in the model.

It is worthwhile to note that in the experiments by Matsuda et al., the concentration of supplied cross-linkers—*N*,*N*′-methylenebis(acrylamide) (MBAA)—is very high, which is 100 mol % with respect to the monomer.[21] In stark contrast, cross-linker concentration for synthesizing conventional hydrogels is often around 1.0 mol % relative to the monomer, which is 2 orders of magnitude lower than the cross-linkers fed to the self-growing hydrogels. It can be inferred that not all bifunctional MBAA cross-linkers are fully reacted (namely, both double bonds are opened); otherwise, the average number of monomers on polymer chains of the newly formed network is about 0.5, which is obviously irrational. For this reason, as depicted in Figure 1d, it is speculated that many MBAA cross-linkers are incompletely reacted (i.e., only one double bond is opened) and are incorporated into polymer chains like monomers, contributing to the number of links of the chain (i.e., chain length), while only a fraction of MBAA cross-linkers is fully reacted to cross-link the chains into a network. Following the classical polymerization kinetics of polymer chemistry,[46] the chemical kinetics of chain propagation in self-growing hydrogels is described by

$$\frac{\mathrm{d}[c_{\mathrm{li}}]}{\mathrm{d}t} = \frac{k_{\mathrm{pm}}[c_{\mathrm{mo}}][c_{\mathrm{ra}}] + k_{\mathrm{pc}}[c_{\mathrm{cr}}][c_{\mathrm{ra}}]}{\beta} \tag{6}$$

where k_{pm} is the propagation rate of monomers and k_{pc} is the propagation rate of cross-linkers; both describe the rate at which unreacted monomers and cross-linkers are incorporated into polymer chains. $[c_{\mathrm{li}}]$ is the concentration of freely jointed links in the gel, $[c_{\mathrm{mo}}]$ is the concentration of monomers, $[c_{\mathrm{ra}}]$ is the concentration of mechanoradicals, and $[c_{\mathrm{cr}}]$ is the concentration of unreacted cross-linkers, all of which are defined per unit volume of the gel. In addition, β is the number of monomers and incompletely reacted cross-linkers in one freely jointed link. Note that the value of β for a common polymer chain depends on the type of monomer, but chains of the newly formed network in this work are composed of both monomers and incompletely reacted cross-linkers, such that its value is hard to determine. Herein, we take $\beta = 1$ for simplicity.

It is worth noting that following the convention of polymer chemistry, concentrations of reactants and products in eq 6 are highlighted in parentheses (e.g., $[c_{\mathrm{ra}}]$) and have the unit of mol/L (i.e., M). In contrast, to model the mechanical behavior of hydrogels, one needs to define concentrations such as c_{ra} as the number of mechanoradicals per unit volume of the gel, and the unit is $1/\mathrm{m}^3$. Using $[c_{\mathrm{ra}}]$ and c_{ra} as an example, the conversion between these two definitions of concentration is as follows

$$[c_{\mathrm{ra}}] = \frac{c_{\mathrm{ra}}}{10^3 N_{\mathrm{Av}}} \tag{7}$$

where N_{Av} is Avogadro's constant. Equation 7 applies to all concentrations, including $[c_{\mathrm{ra}}]$, $[c_{\mathrm{li}}]$, $[c_{\mathrm{mo}}]$, and $[c_{\mathrm{cr}}]$.

As mentioned above, due to the high concentration of cross-linkers fed to the self-growing hydrogels, some incompletely reacted cross-linkers are incorporated into polymer chains, but some cross-linkers are fully reacted and act as cross-links to form the polymer network. The chemical kinetics of cross-link formation can be expressed as

$$\frac{\mathrm{d}[c_{\mathrm{cl}}]}{\mathrm{d}t} = k_{\mathrm{c}}[c_{\mathrm{cr}}][c_{\mathrm{ra}}] \tag{8}$$

where $[c_{\mathrm{cl}}]$ is the concentration of cross-links of the newly generated network and k_{c} is the cross-linking rate (i.e., the rate at which MBAA cross-linkers convert into cross-links of the network).

The process of the propagation reaction is aborted by the termination of free radicals. Coupling and disproportionation are the two modes of termination. Coupling means that two radicals react to form a covalent bond, combining two growing chains into one chain. Alternatively, a pair of radicals can form two new molecules such that the two growing chains are terminated and become dangling chains by a disproportionation reaction. The termination mode depends on many factors, such as the type of monomer, temperature, etc.[46] The chemical kinetics of both modes is governed by

$$\frac{\mathrm{d}[c_{\mathrm{ra}}]}{\mathrm{d}t} = -2k_{\mathrm{t}}[c_{\mathrm{ra}}]^2 \tag{9}$$

where k_{t} is the termination rate of free radicals.

Equations 5−9 describe the three primary processes of network growth, i.e., mechanoradical generation, chain propagation, and chain termination, and yield the amounts of monomers and cross-linkers incorporated into the newly formed networks. The evolution of $[c_{\mathrm{li}}]$ and $[c_{\mathrm{cl}}]$ during the growing period can be determined by numerically solving eqs 6, 8, and eq 9 as follows. At the beginning of one growing period, initial values of all concentrations are known: $[c_{\mathrm{li}}^0]$ and $[c_{\mathrm{cl}}^0]$ are zero, $[c_{\mathrm{ra}}^0]$ is determined by eqs 5 and 7, and $[c_{\mathrm{mo}}^0]$ and $[c_{\mathrm{cr}}^0]$ depend on the amounts of monomers and cross-linkers supplied. At time t, the increments of $[c_{\mathrm{li}}]$, $[c_{\mathrm{cl}}]$, and $[c_{\mathrm{ra}}]$ (i.e., $\mathrm{d}[c_{\mathrm{li}}]$, $\mathrm{d}[c_{\mathrm{cl}}]$, and $\mathrm{d}[c_{ra}]$) are calculated according to eqs 6,8, and9, respectively, and $\mathrm{d}[c_{\mathrm{mo}}]$ and $\mathrm{d}[c_{\mathrm{cr}}]$ are determined by $\mathrm{d}[c_{\mathrm{mo}}] = -k_{\mathrm{pm}}[c_{\mathrm{mo}}][c_{\mathrm{ra}}]\mathrm{d}t$ and $\mathrm{d}[c_{\mathrm{cr}}] = -k_{\mathrm{pc}}[c_{\mathrm{cr}}][c_{\mathrm{ra}}]\mathrm{d}t$, respectively. It follows that the values of $[c_{\mathrm{li}}]$, $[c_{\mathrm{cl}}]$, $[c_{\mathrm{ra}}]$, $[c_{\mathrm{mo}}]$, and $[c_{cr}]$ can be updated at time $t + \Delta t$. By repeating the above steps, we can obtain the final concentrations, including $[c_{\mathrm{li}}^{\mathrm{f}}]$, $[c_{\mathrm{cl}}^{\mathrm{f}}]$, $[c_{\mathrm{ra}}^{\mathrm{f}}]$, $[c_{\mathrm{mo}}^{\mathrm{f}}]$, and $[c_{\mathrm{cr}}^{\mathrm{f}}]$ at the end of the growing period.

2.3. Deformation of Multi-Network Self-Growing Hydrogels. New chains and networks form after the mechanoradical-triggered self-growth of hydrogels, turning the DN hydrogel into a triple-network hydrogel. The mechanical model of multinetwork (MN) hydrogels that are composed of two or more networks can be employed to describe the mechanical behavior of self-growing hydrogels. Consider an MN hydrogel consisting of i ($i = A, B, C, \cdots$) number of networks. The average unstretched length of a chain of the ith network is $r_i^0 = \sqrt{n_i} l_i$, where n_i is the number of freely jointed links on the chain of the ith network and l_i the length of a link. The stretch of a polymer chain of the ith network can be calculated as $\Lambda_i = r_i/r_i^0 = r_i/\sqrt{n_i} l_i$, where r_i is the current length of the chain under stretch. The free energy of a chain in the ith network can be expressed as

$$w_i = n_i kT\left(\frac{\beta_i}{\tanh\beta_i} + \log\frac{\beta_i}{\sinh\beta_i}\right) \tag{10}$$

https://doi.org/10.1021/acs.macromol.3c00837
Macromolecules XXXX, XXX, XXX−XXX

where k is the Boltzmann constant, T is the temperature in Kelvin scale, $\beta_i = L^{-1}\left(\frac{\Lambda_i}{\sqrt{n_i}}\right)$, and L^{-1} is the inverse Langevin function defined by $L(x) = \coth(x) - \frac{1}{x}$.

To relate the stretches of polymer chains to the deformation of MN hydrogels, we adopt the eight-chain Arruda−Boyce model. MN hydrogels consist of multiple individual networks swollen by water and other networks so that the stretch of polymer chains of MN hydrogels originates from two processes: (i) the swelling of polymer networks by water and other networks to form the hydrogel and (ii) the deformation of the hydrogels due to mechanical loadings. To this end, considering the eight-chain model, the stretch of a chain on the ith network of the MN hydrogel can be calculated as

$$\Lambda_i = C_i^{-1/3}\sqrt{\frac{\lambda_1^2 + \lambda_2^2 + \lambda_3^2}{3}} \quad (i = A, B, C, \cdots) \tag{11}$$

where C_i is the volume fraction of the ith network in the MN hydrogels, λ_1, λ_2, and λ_3 are the three principal stretches of the hydrogel. $C_i^{-1/3}$ represents the stretches caused by the swelling of the ith network by water and other networks while $\sqrt{(\lambda_1^2 + \lambda_2^2 + \lambda_3^2)/3}$ represents the contribution from the deformation of MN hydrogels. Equation 11 indicates that chain stretches of different networks can be distinct because of the different volume fractions of each individual network.

As previously mentioned, N_i is the number of the ith polymer chain per unit volume of the ith network. Therefore, C_iN_i is the number of the ith chain per unit volume of the MN hydrogel. By taking into account eq 10, the free energy density function of the MN hydrogel can be expressed as

$$W = \sum_{i=A,B,C\cdots} C_iN_in_ikT\left(\frac{\beta_i}{\tanh\beta_i} + \log\frac{\beta_i}{\sinh\beta_i}\right) \tag{12}$$

Then, the principal Cauchy stresses of the MN self-growing hydrogel can be calculated as

$$\sigma_1 = \sum_{i=A,B,C\cdots} \frac{C_i^{1/3}N_i\sqrt{n_i}kT\beta_i}{3\Lambda_i}\lambda_1^2 - \Pi \tag{13a}$$

$$\sigma_2 = \sum_{i=A,B,C\cdots} \frac{C_i^{1/3}N_i\sqrt{n_i}kT\beta_i}{3\Lambda_i}\lambda_2^2 - \Pi \tag{13b}$$

$$\sigma_3 = \sum_{i=A,B,C\cdots} \frac{C_i^{1/3}N_i\sqrt{n_i}kT\beta_i}{3\Lambda_i}\lambda_3^2 - \Pi \tag{13c}$$

where Π is the hydrostatic pressure that can be determined by using the boundary conditions. For self-growing hydrogels subject to uniaxial tension, we have $\lambda_1 = \lambda$, $\lambda_2 = \lambda_3 = \frac{1}{\sqrt{\lambda}}$, and $\sigma_2 = \sigma_3 = 0$; then, the true stress σ and nominal stress s of the MN hydrogel can be calculated as follows

$$\sigma = \sum_{i=A,B,C\cdots} \frac{C_i^{1/3}N_i\sqrt{n_i}kT\beta_i}{3\Lambda_i}(\lambda^2 - \lambda^{-1}) \tag{14a}$$

$$s = \sum_{i=A,B,C\cdots} \frac{C_i^{1/3}N_i\sqrt{n_i}kT\beta_i}{3\Lambda_i}(\lambda - \lambda^{-2}) \tag{14b}$$

During the first loading−unloading cycle prior to growth, the self-growing hydrogel reported by Matsuda et al.[21] contains two networks, namely, networks A and B. Substituting eqs 1a, 1b into 14b and considering the volume conservation conditions that $N_An_Av_A = 1$ and $N_{B0}n_{B0}v_B = 1$, the nominal stress of the DN hydrogel can be obtained as

$$s = \left(\frac{C_B^{1/3}kT\beta_B}{3v_B\sqrt{n_{B0}}\Lambda_B}\exp\left[\left(\frac{1}{2}q_B - p_B\right)(\Lambda_B^{\max} - C_B^{-1/3})\right] + \frac{C_A^{1/3}kT\beta_A}{3v_A\sqrt{n_A}\Lambda_A}\right)(\lambda - \lambda^{-2}) \tag{15}$$

where $v_A = v_B = v$ are the volume of one link in networks A and B, respectively.

2.4. Strengthening of Self-Growing Hydrogel after Growth. As aforementioned, in the experiments of Matsuda et al.,[21] hydrogel samples are cyclically stretched with a 1 h growth period between each two consecutive loading−unloading cycles, as shown in Figure 1e. During the first loading−unloading cycle, large amounts of mechanoradicals are formed in self-growing hydrogels due to chain breakage. Within the incubation time between the first and second cycles, the generated mechanoradicals trigger the polymerization of supplied monomers to form a new network, namely, network C, thereby completing the first growth period of the self-growing hydrogels. The newly formed network C contains short chains that can break in subsequent loading cycles, thus strengthening the self-growing hydrogel. Therefore, the network alteration theory shown in eqs 1a and 1b also applies to network C, that is, $N_C = N_{C0}\exp[-p_C(\Lambda_C^{\max} - C_C^{-1/3})]$, $n_C = n_{C0}\exp[q_C(\Lambda_C^{\max} - C_C^{-1/3})]$. As suggested by eq 15, the initial chain length n_{C0} and volume fraction C_C of network C directly influence the stress−stretch behavior of the network, which can be determined by using the results in Section 2.2 as follows. It is noteworthy that the newly formed network C is attached to network B, which certainly leads to the existence of interplay between the two networks. However, due to the significantly different chain lengths of the two networks, following conventions in previous works,[25−27] we treat them as two independent networks and ignore their interplay.

In this work, we focus on self-growing hydrogels prefed with a monomer/cross-linker solution, which constitutes a closed system. During the growth process, the hydrogel does not exchange matter with surroundings, and the supplied monomers and cross-linkers contained in the solvent of the hydrogel are polymerized to form the new network C. The increase in the volume of polymer networks equals the decrease in the volume of the solvent, so that the hydrogel volume remains constant during the self-growth process. Note that the final concentrations c_{li}^f and c_{cl}^f for the network C can be obtained following the procedure described in Section 2.2. Then, the volume fraction of network C in the hydrogel can be calculated as

$$C_C = vc_{li}^f \tag{16}$$

where v is the volume of one link of chains in the network C.

In a polymer network, a cross-linker that has Φ number of double bonds can cross-link 2Φ chains, and one chain is connected to two cross-links at its two ends. Therefore, the number of chains in a network should be equal to Φ times that

https://doi.org/10.1021/acs.macromol.3c00837
Macromolecules XXXX, XXX, XXX−XXX

Table 1. Key Model Parameters for Self-Growing Hydrogels

parameter (unit)	definition
n_i $i = A, B, \cdots$	number of freely jointed links on a chain (i.e., chain length) of the ith network
n_{i0} $i = B, C, \cdots$	initial number of freely jointed links on a chain (i.e., initial chain length) of the ith network
v (m^3)	volume of a freely jointed link of polymer networks
p_i $i = B, C, \cdots$	damage parameter that characterizes the decrease of chain density of the ith network
q_i $i = B, C, \cdots$	damage parameter that characterizes the increase of chain length of the ith network
C_i $i = A, B, \cdots$	volume fraction of the ith network in the hydrogel
Λ_i $i = A, B, \cdots$	stretch of the ith network
Λ_i^{max} $i = B, C, \cdots$	maximum stretch of the ith network in the loading history
c_{ld} ($1/m^3$)	number of links entering inactive dangling chains per unit volume of the hydrogel
c_{bc} ($1/m^3$)	number of broken chains per unit volume of the hydrogel
k_{pm} ($L \cdot mol^{-1} \cdot s^{-1}$)	propagation rate of monomers
k_{pc} ($L \cdot mol^{-1} \cdot s^{-1}$)	propagation rate of cross-linkers
k_c ($L \cdot mol^{-1} \cdot s^{-1}$)	cross-linking rate of cross-linkers
k_t ($L \cdot mol^{-1} \cdot s^{-1}$)	termination rate of free radicals
$[c_{mo}]$, $[c_{mo}^0]$, $[c_{mo}^f]$ ($mol \cdot L^{-1}$)	current/initial/final molar concentration of supplied monomers per unit volume of the hydrogel during the growth period
$[c_{cr}]$, $[c_{cr}^0]$, $[c_{cr}^f]$ ($mol \cdot L^{-1}$)	current/initial/final molar concentration of supplied cross-linkers per unit volume of the hydrogel during the growth period
$[c_{ra}]$, $[c_{ra}^0]$, $[c_{ra}^f]$ ($mol \cdot L^{-1}$)	current/initial/final molar concentration of free radicals per unit volume of the hydrogel during the growth period
c_{ra} ($1/m^3$)	number of radicals per unit volume of the hydrogel
$[c_{li}]$, $[c_{li}^0]$, $[c_{li}^f]$ ($mol \cdot L^{-1}$)	current/initial/final molar concentration of freely jointed links of the newly formed network per unit volume of the hydrogel during the growth period
c_{li}^f ($1/m^3$)	final number of freely jointed links of the newly formed network per unit volume of the hydrogel at the end of one growth period
$[c_{cl}]$, $[c_{cl}^0]$, $[c_{cl}^f]$ ($mol \cdot L^{-1}$)	current/initial/final molar concentration of cross-links of the newly formed network per unit volume of the hydrogel during the growth period
c_{cl}^f ($1/m^3$)	final number of cross-links of the newly formed network per unit volume of the hydrogel at the end of one growth period
Φ	cross-linker functionality
β	number of monomers and incompletely reacted cross-linkers in one freely jointed link

of cross-links. For the newly formed network C, in a unit volume of the self-growing hydrogel, the number of cross-links of network C is c_{cl}^f; hence, the number of chains of network C is Φc_{cl}^f. Considering that the number of links of network C per unit volume of the gel is c_{li}^f, the chain length of the newly formed network C can thus be determined as

$$n_{C0} = \frac{c_{li}^f}{\Phi c_{cl}^f} \tag{17}$$

where the value of Φ depends on the cross-linker functionality. In the experiments of Matsuda et al.,[21] the cross-linker used is MBAA, which contains two C=C double bonds, such that $\Phi = 2$.

Because the new network C comes from the internal solvent of the self-growing hydrogel, its formation does not affect the mechanical behaviors of networks A and B. For example, the volume fractions of networks A and B and the maximum stretch of network B in the loading history Λ_B^{max} are not influenced by the formation of network C. As we discussed above, the newly formed network C should serve the role of a brittle network (Figure 1c) that then breaks during subsequent deformation to trigger further network formation; the mechanical behavior of network C is the same as that of network B and can therefore be described by the network alteration model. To this end, the nominal stress of the self-growing hydrogel after first growth—which contains networks A, B, and C—can be expressed as

$$s = \left(\frac{C_A^{1/3} kT\beta_A}{3v\sqrt{n_A}\Lambda_A} + \sum_{i=B,C} \frac{C_i^{1/3} kT\beta_i}{3v\sqrt{n_{i0}}\Lambda_i} \exp\left[\left(\frac{1}{2} q_i - p_i \right) (\Lambda_i^{max} - C_i^{-1/3}) \right] \right) (\lambda - \lambda^{-2}) \tag{18}$$

From eq 18, it can be concluded that during the second loading, if the stretch does not exceed the maximum stretch level of the first loading cycle, then only network C breaks to generate mechanoradicals and trigger subsequent network formation. Otherwise, both networks B and C contribute to mechanoradical generation and the formation of a new network.

After the second loading/unloading cycle, the hydrogel undergoes the second self-growth in the presence of remaining monomers and cross-linkers in the hydrogel solvent, forming a new network D. The mechanical response of the hydrogel after second growth—which consists of networks A, B, C, and D—can be derived according to the procedure described in Section 2. The growth process of self-growing hydrogels can be repeated until the monomers/cross-linkers are completely consumed or the hydrogel is fractured.

For convenience, parameters of the chemomechanical model to describe the growth and deformation of self-growing hydrogels are summarized in Table 1.

3. RESULTS AND DISCUSSION

In this section, the chemomechanical model presented in Section 2 is applied to simulate the growth and strengthening of self-growing hydrogels—these hydrogels are subjected to cyclic stretching with a 1 h growth time between every two consecutive loading−unloading cycles.[21] Key aspects of the

https://doi.org/10.1021/acs.macromol.3c00837
Macromolecules XXXX, XXX, XXX−XXX

growth process, including chain-rupture-induced mechanoradical generation, polymerization of monomers and cross-linkers, the formation of the new network, and its influence on the mechanical behavior of self-growing hydrogels, are analyzed. Unless otherwise stated, the values of model parameters given in Table 2 are used in numerical simulations in this section.

Table 2. Values of Key Model Parameters Used in This Work

n_A	n_{B0}	v (m^3)	C_A
5000[21]	50[21]	1.8×10^{-28}[33]	0.067[33]
C_B	k_{pm}, k_{pc}, k_p ($L \cdot mol^{-1} \cdot s^{-1}$)	k_t ($L \cdot mol^{-1} \cdot s^{-1}$)	k_c ($L \cdot mol^{-1} \cdot s^{-1}$)
0.033[33]	1×10^{4}[46]	1×10^{4}[46]	1.7×10^{2}[46]
$[c_{cr}^0]$ ($mol \cdot L^{-1}$)	$[c_{mo}^0]$ ($mol \cdot L^{-1}$)	p_B	q_B
0.072[21]	0.072[21]	0.1743	0.174

3.1. Concentration of Mechanoradicals. Force-induced chain scission and the associated mechanoradical generation are the triggers that initiate the formation of a new network. As reported by Matsuda et al.,[21] the concentration of mechanoradicals significantly affects the growth process of DN hydrogels. Herein, by using eq 5, we study the effects of key model parameters on the concentration of mechanoradicals, including the volume fraction C_B of network B, the value of $p_B - q_B$, and the maximum stretch Λ_B^{max} of network B. For a DN hydrogel subject to uniaxial tension during the first loading, $\Lambda_B^{max} = C_B^{-1/3}\sqrt{(\lambda^2 + 2\lambda^{-1})/3}$, where λ represents the uniaxial stretch applied to the hydrogel. Figures 2a and 2b illustrate the influence of $p_B - q_B$ and C_B on mechanoradical generation, respectively. Both plots show that the concentration of mechanoradicals increases with increasing stretch, as higher stretches break more polymer chains and thus produce more mechanoradicals. As indicated by eq 5, it is not the absolute values of p_B and q_B that determine the concentration of mechanoradicals but the difference between them. In Figure 2a, we take $C_B = 0.033$. Figure 2a shows that the concentration of mechanoradicals increases as the value of $p_B - q_B$ increases, since a higher $p_B - q_B$ means that more links enter the inactive dangling chains, indicating a higher degree of chain breakage. For Figure 2b, we use $p_B - q_B = 0.0003$ and fix the volume fraction of polymer networks of the gel, i.e., $C_A + C_B = 0.1$. It is found that increasing the volume fraction of network B leads to higher mechanoradical concentrations because, with increasing volume fraction of network B, the number of broken chains per unit volume of the gel increases, yielding more mechanoradicals generated.

Notably, Matsuda et al. report that the mechanoradical concentration in fully necked DN hydrogels is estimated to be of the order of 10^{-5} M (i.e., mol/L),[21] which is highlighted as the light blue region in Figure 2. At the same level of stretch (i.e., $\lambda = 5.7$), our model essentially predicts mechanoradical concentrations of the same order of magnitude as the experimental measurements. To this end, in the following section of this paper, we choose $p_B - q_B = 0.0003$ and $C_B = 0.033$ for all numerical simulations, which gives the initial mechanoradical concentration $[c_{ra}^0] = 2.8 \times 10^{-5}$ M at $\lambda = 6$.

3.2. Chemical Kinetics of the Polymerization of Monomers and Cross-Linkers. The polymerization of monomers and cross-linkers takes place when dissociative monomers and cross-linkers meet mechanoradicals, which eventually leads to the formation of the new network. The chemical kinetics of the process—which is governed by eqs 6, 8, and 9 presented in Section 2—is mainly determined by four parameters, including the propagation rate of the monomer k_{pm}, the propagation rate of the cross-linker k_{pc}, the cross-linking rate of the cross-linker k_c, and the termination rate of radicals k_t. In this work, we set $k_{pm} = k_{pc} = k_p$ for simplicity.

In Figure 3, we plot the concentration−time profiles of various reaction rates during the first growth period of 1 h (Figure 1e). As mentioned above, based on the simulation results in Section 3.1 and the experiments of Matsuda et al.,[21] the initial mechanoradical concentration $[c_{ra}^0] = 2.8 \times 10^{-5}$ M is used here. In Figure 3a, given the values of k_p, k_c, and k_t, the total concentration of links on polymer chains in the new network C (i.e., $[c_{li}]$) is plotted as a function of the growth time. It is clear that $[c_{li}]$ increases rapidly in the early stages of growth and gradually saturates, indicating that most of the reactions occur in the early stages of growth. In Figure 3a, three curves with comparatively large k_p (i.e., red, blue, and yellow curves) have nearly the same $[c_{li}^f]$ at the end of the 1 h growing period, with a value of about 0.14 M. Note that as shown in Table 2, the sum of $[c_{mo}^0]$ and $[c_{cr}^0]$ is 0.144 M. That is, for these three cases of large k_p, monomers and cross-linkers are almost fully consumed within 1 h because of the high rate of monomer and cross-linker incorporation into polymer chains. We take the red curve (with $k_p = 1 \times 10^4$ $L \cdot mol^{-1} \cdot s^{-1}$, $k_t = 1 \times 10^4$ $L \cdot mol^{-1} \cdot s^{-1}$, and $k_c = 2 \times 10^2$ $L \cdot mol^{-1} \cdot s^{-1}$) as the baseline case and compare it with the other three cases to assess the effects of reaction rates on the polymerization process. The comparison between the red and green curves shows that a larger k_p leads to higher $[c_{li}]$ because more monomers and cross-linkers participate in the polymerization

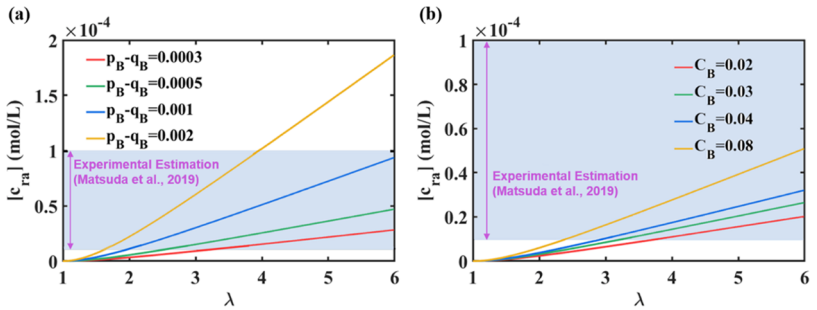

Figure 2. Simulation results of mechanoradical concentration as a function of applied stretch. (a) Concentration−stretch curves with various values of $p_B - q_B$. (b) Concentration−stretch curves with different volume fractions of network B.

https://doi.org/10.1021/acs.macromol.3c00837
Macromolecules XXXX, XXX, XXX−XXX

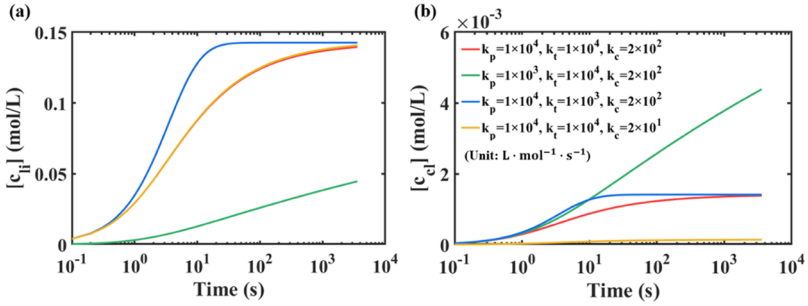

Figure 3. Simulation results of the concentration of freely jointed links and cross-links on polymer chains of newly formed networks. (a) Evolution of link concentration $[c_{li}]$ over the 1 h growth time for various reaction rates (the red line and the yellow line are almost overlapped). (b) Evolution of cross-link concentration $[c_{cl}]$ over time for various reaction rates.

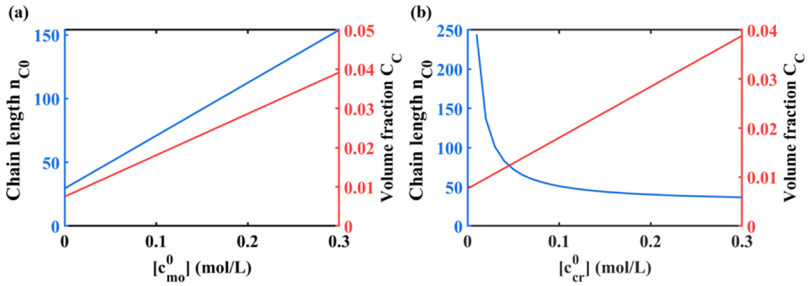

Figure 4. Effects of initial monomer/cross-linker concentrations on the chain length and volume fraction of the newly formed network C. (a) Resulting chain length and volume fraction of network C after 1 h growth as a function of initial monomer concentration $[c^0_{mo}]$. In making this plot, $[c^0_{cr}]$ is set to 0.072 M. (b) Resulting chain length and volume fraction of network C after 1 h growth as a function of initial cross-linker concentration $[c^0_{cr}]$. For this plot, $[c^0_{mo}]$ is set to 0.072 M.

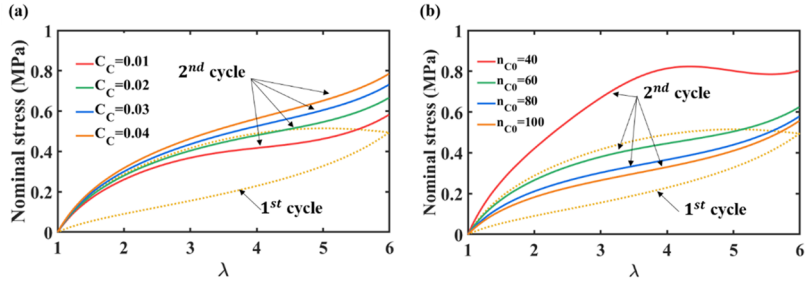

Figure 5. Strengthened mechanical behavior of self-growing hydrogels after 1st growth. (a) Stress−stretch curves of self-growing hydrogels with different volume fractions C_C. (b) Stress−stretch curves of self-growing hydrogels with different chain lengths n_{C0}.

reaction before all free radicals are terminated. Comparing the red and blue curves indicates that a lower k_t causes the concentration to change more drastically at the beginning, thus reaching equilibrium faster because a lower k_t allows more radicals to participate in polymerization reactions before their termination. Moreover, the red and yellow curves almost overlap, indicating that k_c has little effect on $[c_{li}]$ since k_c is several orders of magnitude lower than the value of k_p in the model.

As mentioned earlier, the incompletely reacted cross-linkers are incorporated into the polymer chains as links, while fully reacted cross-linkers become cross-links. In Figure 3b, the variation of cross-link concentration $[c_{cl}]$ with time is presented. We also take the red curve ($k_p = 1 \times 10^4$ L·mol^{-1}·s^{-1}, $k_t = 1 \times 10^4$ L·mol^{-1}·s^{-1}, and $k_c = 2 \times 10^2$ L·mol^{-1}·s^{-1}) as the baseline case. When varying k_p to a smaller value (from the red curve to the green one), fewer cross-linkers are incorporated into polymer chains as links so that more cross-links are formed, resulting in higher $[c_{cl}]$. Reducing k_t—from the red curve to the blue one—causes the concentration $[c_{cl}]$ to change more sharply at early stages of growth and saturate faster as more radicals are involved in the polymerization reaction. When k_c is decreased from 2×10^2 L·mol^{-1}·s^{-1} (the red curve) to 2×10^1 L·mol^{-1}·s^{-1} (the yellow curve), fewer cross-linkers are fully reacted so that the plateau of the yellow curve becomes much lower. Besides, the initial concentrations of monomer and cross-linker (i.e., $[c^0_{mo}]$ and $[c^0_{cr}]$) affect the chemical kinetics of the polymerization process as well (Figure S1).

3.3. New Network Generated during Self-Growth. A new network C is formed due to the polymerization of monomers and cross-linkers in the hydrogel solvent. According to eqs 16 and17, the volume fraction C_C and chain length n_{C0} of the newly formed network can be evaluated by using the results in Section 3.2. In this regard, the structure of the new network can be adjusted by changing the initial concentrations of monomer and cross-linker (i.e., $[c^0_{mo}]$ and $[c^0_{cr}]$). Figure 4a shows that when fixing $[c^0_{cr}]$ to 0.072 M, both the chain length and volume fraction of the new network are linearly proportional to $[c^0_{mo}]$ after the 1 h growth period. In making

https://doi.org/10.1021/acs.macromol.3c00837
Macromolecules XXXX, XXX, XXX−XXX

Figure 4b, we set $[c_{mo}^0] = 0.072$ M. It shows that after the 1 h growth period, the volume fraction of the new network increases linearly with increasing $[c_{cr}^0]$. Moreover, the chain length n_{C0} of the new network C decreases rapidly and gradually approaches a stable value as $[c_{cr}^0]$ increases. It is worth noting that for $[c_{cr}^0] = [c_{mo}^0] = 0.072$ M— consistent with the values used in the experiments of Matsuda et al.,[21] the newly formed network C accounts for 1.51% of the gel volume, and the initial chain length n_{C0} is about 59.

3.4. Stress−Stretch Response of the Gel after Self-Growth. After the formation of network C during the self-growth process, the hydrogel became a triple-network hydrogel. According to eq 18, the network properties, including the initial chain length n_{C0} and the volume fraction C_C of network C, directly affect the stress−stretch behavior of the self-growing hydrogel. Figures 5a and5b plot the nominal stress−stretch curves of hydrogels with different initial chain lengths n_{C0} and volume fraction C_C, respectively. As mentioned above, the material parameters displayed in Table 2 are adopted in the numerical simulations. The yellow dashed lines represent the stress response of the DN hydrogel in the first loading−unloading cycle before self-growth, showing a large hysteresis loop that indicates significant energy dissipation due to chain breakage. The other solid curves correspond to the stresses of the hydrogel during second loading after first growth.

In making Figure 5a, n_{C0} is fixed to 59, and it can be seen that after growth, the gel exhibits higher strength and modulus at the second loading than at the first unloading. In addition, the higher the volume fraction C_C of the newly formed network C, the higher the strength and modulus, since a higher C_C indicates that there are more chains per unit volume of the hydrogel to bear forces. Figure 5b discusses the effect of the initial chain length n_{C0}, where $C_C = 0.0151$. Network C with longer chains leads to lower hydrogel strength, while network C with shorter chains results in enhanced hydrogel strength but more pronounced softening because short chains easily approach their stretch limit, thereby increasing the stress level of the hydrogel but causing the gel to soften.[33] Similarly, other factors, like mechanoradical concentration, initial concentration of monomers and cross-linkers, etc., can also affect the stress−stretch behaviors of the self-growing hydrogel after growth. The results and discussions are presented in the Supporting Information (Figures S2−S5).

4. STRENGTHENING OF SELF-GROWING HYDROGELS SUBJECT TO REPETITIVE STRETCHING AND GROWTH

Matsuda et al. showed that DN gels could grow sustainably in strength and size under repetitive stretching with a continuous supply of monomers and cross-linkers.[21] To demonstrate the idea, the researchers conducted two sets of experiments. In the first set of experiments, DN gels were prefed with a mixed solution of monomer and cross-linker before testing but were not immersed in the solution anymore during the repetitive stretching and growing process. During the experiments, there was no exchange of substances between the hydrogel and its surroundings, forming a closed system. As for the second set of experiments, they performed repeated stretching of DN gels that were immersed in the mixed solution of monomers and cross-linkers all of the time, such that the monomers, cross-linkers, and water molecules could diffuse into the gel and change the gel volume, component concentrations, and the reference state continuously, which yielded an open system. Therefore, a fully coupled diffusion and growth model needs to be established to simulate the open system, which is more complicated than the closed system. Note that the chemo-mechanical model developed in Section 2 only holds for the closed system. The open system will be investigated in our future work. Herein, we focus on the self-growth of the closed system. According to the experiments of Matsuda et al.,[21] the closed-system hydrogels underwent four loading−unloading cycles (each with a maximum stretch of 6), with a growing time of 1 h between two consecutive cycles. It was revealed that the first growth leads to a significant stress increase during the second loading, and the stress−stretch curve of the self-growing hydrogel shows a large hysteresis loop in the second loading−unloading cycle. However, the second growth merely causes a slight stress increase in the third loading compared to the stress−stretch curve of the second unloading.[21] Similarly, the effect of third growth is also negligible.

To understand the experimental findings of Matsuda et al.[21] and to validate our chemomechanical model, we next simulate the mechanical behaviors of the closed-system self-growing hydrogels over loading−unloading cycles using the chemo-mechanical theory presented in Section 2. According to Matsuda et al., the stress−stretch curves of the third and fourth cycles in the experiments are very similar, such that we only study the first three cycles in the simulations. In order to relate the simulation results to the experiments of Matsuda et al., the key model parameters used in the simulations are as follows: In the experiments,[21] the concentrations of monomers and cross-linkers in the mixed solution are both 0.08 M because the concentrations of monomer and cross-linker in the internal and external solutions are consistent.[48] In the modeling, the initial volume fraction of the polymer network is $C_A + C_B = 0.1$ (Table 2), so the initial concentrations of monomers and cross-linkers per unit volume of the DN gel are both $0.08\ \text{M} \times (1 - C_A - C_B) = 0.072$ M. The maximum stretch of each loading is set to $\lambda_{max} = 6$ in accordance with the experiments, so that in the nth loading−unloading cycle, only the new network generated in the $(n-1)^{th}$ growth period ruptures and produces mechanoradicals. As mentioned above, q_i and p_i are two damage parameters that determine the degree of damage of the polymer network and can be obtained by fitting the experimental data.[49] After fitting to the experimentally measured mechanoradical concentration in the first cycle, we obtain $p_i - q_i = 3 \times 10^{-4}$ (Figure 2). However, due to the lack of experimental data in the second and third cycles, we keep the value of $p_i - q_i$ the same in the second and third cycles for simplicity. By setting $p_i - q_i = 3 \times 10^{-4}$ for each network of the self-growing hydrogel, we can readily calculate the concentration of mechanoradicals at the beginning of each growth period. Elastomers and hydrogels of different chain lengths have different damage parameters.[49] As for self-growing hydrogels, polymer networks with shorter chain lengths and higher chain densities face more pronounced damage, thereby possessing higher damage parameters. We try to fit the experimentally measured stress−stretch behaviors, especially the ultimate stresses at the maximum stretch of $\lambda = 6$. It is found that the three sets of parameters in Table 3 give theoretical predictions consistent with the experimental measurements by Matsuda et al.[21] (Figure 6b). Based on the experiments, the growth time between two consecutive loading−unloading cycles is taken to be 1 h. The formation of network C and its influence are extensively discussed in

https://doi.org/10.1021/acs.macromol.3c00837
Macromolecules XXXX, XXX, XXX−XXX

Table 3. Damage Parameters for Networks B, C, and D

q_B	p_B	q_C	p_C	q_D	p_D
0.174	0.1743	0.19	0.1903	0.02	0.0203

Section 2. Similarly, the network structure and mechanical behavior of network D formed during the second growth can be obtained by following the procedures presented in Section 2. In the following, we use our chemomechanical theory to obtain the stress−stretch curves of self-growing gels in cyclic loading−unloading cycles and validate our theoretical model by comparing the theoretical predictions to the experimental results of Matsuda et al.[21]

Figure 6 shows the cyclic loading−unloading curves of self-growing hydrogels of the closed system obtained from simulations and quantitatively compares the stresses at $\lambda = 6$ of self-growing hydrogels predicted by theoretical modeling to that experimentally measured by Matsuda et al.[21] Our model captures the following main features of the growth process of self-growing hydrogels, which is in good agreement with the experimental observations of Matsuda et al.[21]

- As presented in Figure 6a, the first loading−unloading cycle has a large hysteresis loop, indicating the destruction of the sacrificial network B. Meanwhile, many mechanoradicals are generated to trigger self-growth in the next growth period.
- Network C is formed during the first growth of 1 h between the first and second loading−unloading cycles. After the first growth, the hydrogel exhibits higher modulus and strength during the second loading than the damaged DN gel during the first unloading, implying that the gel is strengthened due to the newly formed network C during the first growth. In addition, the large hysteresis loop that appears during the second loading−unloading cycle demonstrates that the newly formed network C is brittle, which breaks and generates mechanoradicals as well.
- After the second 1 h growth period between the second and third loading−unloading cycles, the mechanical properties of the hydrogels do not show noticeable enhancement during the third loading−unloading process. The stress−stretch curve almost overlaps with the unloading curve of the second loading−unloading cycle, which indicates that the hydrogel is hardly strengthened during the second growth. This is because the closed system contains only finite monomers and cross-linkers, which are almost completely consumed during the first growth, such that a limited amount of monomers and cross-linkers participate in the new network formation during the second growth, giving rise to only slight growth.
- We calculate the energy dissipation ratio of each cycle, which is defined as the ratio of energy dissipated to work done in each cycle. They are 47.4% in the first cycle, 30.8% in the second cycle, and 2.2% in the third cycle, respectively. The energy dissipation ratio decreases over cycles, with the energy dissipation ratio in the third cycle being much smaller than that of the first two cycles.
- Figure 6b shows the ultimate stresses at $\lambda = 6$ in Matsuda's experiments and our theoretical modeling. We first obtain the results that the experimentally measured ultimate forces at $\lambda = 6$ in the first three cycles are 1.49, 1.85, and 1.92 N, respectively. The dimensions of the sample's cross section are 1.5 mm in thickness and 2 mm in width. Then, the corresponding ultimate stresses in each cycle can be calculated, which are 0.497, 0.617, and 0.640 MPa, respectively. Meanwhile, the ultimate stresses predicted by our theoretical model are 0.494, 0.627, and 0.651 MPa, respectively, for the three consecutive cycles. The experimentally measured and theoretically predicted ultimate stresses are pretty close, which demonstrates that our model can accurately capture the important features of the growth process of the self-growing hydrogels.

5. CONCLUSIONS

In this work, we develop a chemomechanical model for the study of a mechanoresponsive self-growing hydrogel, an emerging polymeric material that can self-grow and strengthen under repeated mechanical stresses. Based on the chain alteration model for DN hydrogels, we put forward a quantitative expression for the generation of mechanoradicals and combine it with the chemical kinetics of new network polymerization initiated by mechanoradicals, eventually obtaining the chemomechanical model of self-growing hydrogels. Through systematic parametric studies, we quantitatively illustrate the significance of key factors that affect the self-growing process of hydrogels, such as the concentration of mechanoradicals, the reaction rates of monomers and cross-linkers in the presence of mechanoradicals, etc. Finally, we quantitatively predict the strengthened mechanical behavior of self-growing hydrogels over repetitive stretching and growth. The results are in good agreement with the observations in the experiments.[21] This work quantitatively reveals the chemo-

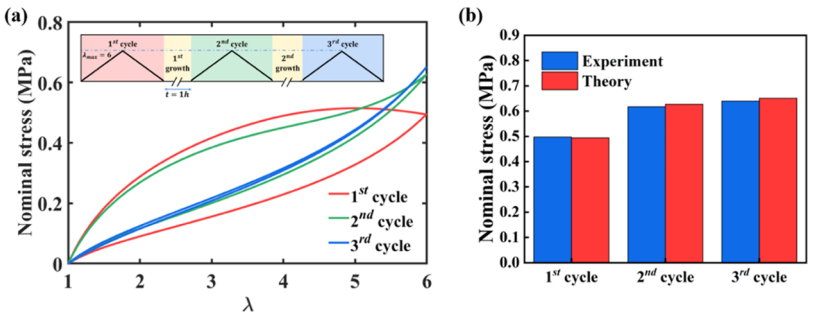

Figure 6. Strengthening and self-growing behaviors of hydrogels subjected to repetitive stretching and growth. (a) Stress−stretch curves of self-growing hydrogels subjected to repetitive stretching and growth. Insets: time profiles of the repetitive stretching and growth of self-growing hydrogels. (b) Comparison of ultimate stresses between theory and experiment at the maximum stretch $\lambda = 6$ in cyclic loading−unloading tests.

https://doi.org/10.1021/acs.macromol.3c00837
Macromolecules XXXX, XXX, XXX−XXX

mechanics underpinning the growth and strengthening of self-growing hydrogels.

■ ASSOCIATED CONTENT

Supporting Information

The Supporting Information is available free of charge at https://pubs.acs.org/doi/10.1021/acs.macromol.3c00837.

Initial monomer and cross-linker concentrations; effects of mechanoradical concentration on the stress−stretch response of the self-growing hydrogel after self-growth; effects of reaction rates on the stress−stretch response of the self-growing hydrogel after self-growth; effects of the initial monomer and cross-linker concentrations on the stress−stretch response of the self-growing hydrogel after self-growth (PDF)

■ AUTHOR INFORMATION

Corresponding Author

Zheng Jia − *State Key Laboratory of Fluid Power and Mechatronic Systems, Key Laboratory of Soft Machines and Smart Devices of Zhejiang Province, Center for X-Mechanics, Department of Engineering Mechanics, Zhejiang University, Hangzhou 310027, China;* orcid.org/0000-0001-8459-515X; Email: zheng.jia@zju.edu.cn

Authors

Zhi Sheng − *State Key Laboratory of Fluid Power and Mechatronic Systems, Key Laboratory of Soft Machines and Smart Devices of Zhejiang Province, Center for X-Mechanics, Department of Engineering Mechanics, Zhejiang University, Hangzhou 310027, China*

Jie Ma − *State Key Laboratory of Fluid Power and Mechatronic Systems, Key Laboratory of Soft Machines and Smart Devices of Zhejiang Province, Center for X-Mechanics, Department of Engineering Mechanics, Zhejiang University, Hangzhou 310027, China*

Zihang Shen − *State Key Laboratory of Fluid Power and Mechatronic Systems, Key Laboratory of Soft Machines and Smart Devices of Zhejiang Province, Center for X-Mechanics, Department of Engineering Mechanics, Zhejiang University, Hangzhou 310027, China*

Shaoxing Qu − *State Key Laboratory of Fluid Power and Mechatronic Systems, Key Laboratory of Soft Machines and Smart Devices of Zhejiang Province, Center for X-Mechanics, Department of Engineering Mechanics, Zhejiang University, Hangzhou 310027, China;* orcid.org/0000-0002-1217-4644

Complete contact information is available at: https://pubs.acs.org/10.1021/acs.macromol.3c00837

Notes

The authors declare no competing financial interest.

■ ACKNOWLEDGMENTS

This work is supported by the National Key Technologies Research and Development Program (Grant No. 2022YFC3203900), the Natural Science Foundation of Zhejiang Province (Grant No. LR22A020005), the National Natural Science Foundation of China (Grant No. 12072314), and the 111 Project (Grant No. B21034).

■ REFERENCES

(1) Suzuka, J.; Tsuda, M.; Wang, L.; Kohsaka, S.; Kishida, K.; Semba, S.; Sugino, H.; Aburatani, S.; Frauenlob, M.; Kurokawa, T.; Kojima, S.; Ueno, T.; Ohmiya, Y.; Mano, H.; Yasuda, K.; Gong, J. P.; Tanaka, S. Rapid Reprogramming of Tumour Cells into Cancer Stem Cells on Double-Network Hydrogels. *Nat. Biomed. Eng.* **2021**, *5*, 914−925.

(2) Xu, S.; Li, H.; Ding, H.; Fan, Z.; Pi, P.; Cheng, J.; Wen, X. Allylated Chitosan-Poly(N-Isopropylacrylamide) Hydrogel Based on a Functionalized Double Network for Controlled Drug Release. *Carbohydr. Polym.* **2019**, *214*, 8−14.

(3) Nonoyama, T.; Wada, S.; Kiyama, R.; Kitamura, N.; Mredha, M. T. I.; Zhang, X.; Kurokawa, T.; Nakajima, T.; Takagi, Y.; Yasuda, K.; Gong, J. P. Double-Network Hydrogels Strongly Bondable to Bones by Spontaneous Osteogenesis Penetration. *Adv. Mater.* **2016**, *28*, 6740−6745.

(4) Yang, F.; Zhao, J.; Koshut, W. J.; Watt, J.; Riboh, J. C.; Gall, K.; Wiley, B. J.; Yang, F.; Zhao, J.; Wiley, B. J.; Koshut, W. J.; Gall, K.; Watt, J.; Riboh, J. C. A Synthetic Hydrogel Composite with the Mechanical Behavior and Durability of Cartilage. *Adv. Funct. Mater.* **2020**, *30*, No. 2003451.

(5) Jiao, Q.; Cao, L.; Zhao, Z.; Zhang, H.; Li, J.; Wei, Y. Zwitterionic Hydrogel with High Transparency, Ultrastretchability, and Remarkable Freezing Resistance for Wearable Strain Sensors. *Biomacromolecules* **2021**, *22*, 1220−1230.

(6) Wang, C.; Chen, X.; Wang, L.; Makihata, M.; Liu, H. C.; Zhou, T.; Zhao, X. Bioadhesive Ultrasound for Long-Term Continuous Imaging of Diverse Organs. *Science* **2022**, *377*, 517−523.

(7) Zhang, H.; Niu, W.; Zhang, S. Extremely Stretchable, Sticky and Conductive Double-Network Ionic Hydrogel for Ultra-Stretchable and Compressible Supercapacitors. *Chem. Eng. J.* **2020**, *387*, No. 124105.

(8) Liu, C.; Morimoto, N.; Jiang, L.; Kawahara, S.; Noritomi, T.; Yokoyama, H.; Mayumi, K.; Ito, K. Tough Hydrogels with Rapid Self-Reinforcement. *Science* **2021**, *372*, 1078−1081.

(9) Kim, J.; Zhang, G.; Shi, M.; Suo, Z. Fracture, Fatigue, and Friction of Polymers in Which Entanglements Greatly Outnumber Cross-Links. *Science* **2021**, *374*, 212−216.

(10) Wang, Z.; Zheng, X.; Ouchi, T.; Kouznetsova, T. B.; Beech, H. K.; Av-Ron, S.; Matsuda, T.; Bowser, B. H.; Wang, S.; Johnson, J. A.; Kalow, J. A.; Olsen, B. D.; Gong, J. P.; Rubinstein, M.; Craig, S. L. Toughening Hydrogels through Force-Triggered Chemical Reactions That Lengthen Polymer Strands. *Science* **2021**, *374*, 193−196.

(11) Gong, J. P.; Katsuyama, Y.; Kurokawa, T.; Osada, Y. Double-Network Hydrogels with Extremely High Mechanical Strength. *Adv. Mater.* **2003**, *15*, 1155−1158.

(12) Gong, J. P. Why Are Double Network Hydrogels so Tough? *Soft Matter* **2010**, *6*, 2583−2590.

(13) Chen, Q.; Zhu, L.; Chen, H.; Yan, H.; Huang, L.; Yang, J.; Zheng, J. A Novel Design Strategy for Fully Physically Linked Double Network Hydrogels with Tough, Fatigue Resistant, and Self- Healing Properties. *Adv. Funct. Mater.* **2015**, *25*, 1598−1607.

(14) Sun, J. Y.; Zhao, X.; Illeperuma, W. R. K.; Chaudhuri, O.; Oh, K. H.; Mooney, D. J.; Vlassak, J. J.; Suo, Z. Highly Stretchable and Tough Hydrogels. *Nature* **2012**, *489*, 133−136.

(15) Jiang, X.; Xiang, N.; Wang, J.; Zhao, Y.; Hou, L. Preparation and Characterization of Hybrid Double Network Chitosan/Poly-(Acrylic Amide-Acrylic Acid) High Toughness Hydrogel through Al3+ Crosslinking. *Carbohydr. Polym.* **2017**, *173*, 701−706.

(16) Wang, Y.; Xue, Y.; Wang, J.; Zhu, Y.; Zhu, Y.; Zhang, X.; Liao, J.; Li, X.; Wu, X.; Qin, Y. X.; Chen, W. A Composite Hydrogel with High Mechanical Strength, Fluorescence, and Degradable Behavior for Bone Tissue Engineering. *Polymers* **2019**, *11*, No. 1112, DOI: 10.3390/polym11071112.

(17) Tuncaboylu, D. C.; Argun, A.; Algi, M. P.; Okay, O. Autonomic Self-Healing in Covalently Crosslinked Hydrogels Containing Hydrophobic Domains. *Polymer* **2013**, *54*, 6381−6388.

(18) Xu, X.; Jerca, V. V.; Hoogenboom, R. Bioinspired Double Network Hydrogels: From Covalent Double Network Hydrogels via

Hybrid Double Network Hydrogels to Physical Double Network Hydrogels. *Mater. Horiz.* **2021**, *8*, 1173−1188.
(19) Chen, Q.; Zhu, L.; Huang, L.; Chen, H.; Xu, K.; Tan, Y.; Wang, P.; Zheng, J. Fracture of the Physically Cross-Linked First Network in Hybrid Double Network Hydrogels. *Macromolecules* **2014**, *47*, 2140−2148.
(20) Liu, S.; Li, K.; Hussain, I.; Oderinde, O.; Yao, F.; Zhang, J.; Fu, G. A Conductive Self-Healing Double Network Hydrogel with Toughness and Force Sensitivity. *Chem. - Eur. J.* **2018**, *24*, 6632−6638, DOI: 10.1002/chem.201800259.
(21) Matsuda, T.; Kawakami, R.; Namba, R.; Nakajima, T.; Gong, J. P. Mechanoresponsive Self-Growing Hydrogels Inspired by Muscle Training. *Science* **2019**, *363*, 504−508.
(22) Baytekin, H. T.; Baytekin, B.; Grzybowski, B. A. Mechanoradicals Created in "Polymeric Sponges" Drive Reactions in Aqueous Media. *Angew. Chem. Int. Ed.* **2012**, *51*, 3596−3600.
(23) Baytekin, H. T.; Baytekin, B.; Huda, S.; Yavuz, Z.; Grzybowski, B. A. Mechanochemical Activation and Patterning of an Adhesive Surface toward Nanoparticle Deposition. *J. Am. Chem. Soc.* **2015**, *137*, 1726−1729.
(24) Xin, A.; Du, H.; Yu, K.; Wang, Q. Mechanics of Bacteria-Assisted Extrinsic Healing. *J. Mech. Phys. Solids* **2020**, *139*, No. 103938.
(25) Wang, Q.; Gao, Z.; Yu, K. Interfacial Self-Healing of Nanocomposite Hydrogels: Theory and Experiment. *J. Mech. Phys. Solids* **2017**, *109*, 288−306.
(26) Yu, K.; Xin, A.; Wang, Q. Mechanics of Self-Healing Polymer Networks Crosslinked by Dynamic Bonds. *J. Mech. Phys. Solids* **2018**, *121*, 409−431.
(27) Yu, K.; Xin, A.; Wang, Q. Mechanics of Light-Activated Self-Healing Polymer Networks. *J. Mech. Phys. Solids* **2019**, *124*, 643−662.
(28) Tang, J.; Chen, X.; Pei, Y.; Fang, D. Pseudoelasticity and Nonideal Mullins Effect of Nanocomposite Hydrogels. *J. Appl. Mech.* **2016**, *83*, No. 111010.
(29) Wang, Q.; Gao, Z. A Constitutive Model of Nanocomposite Hydrogels with Nanoparticle Crosslinkers. *J. Mech. Phys. Solids* **2016**, *94*, 127−147.
(30) Yu, K.; Feng, Z.; Du, H.; Wang, Q. Mechanics of Photosynthesis Assisted Polymer Strengthening. *J. Mech. Phys. Solids* **2021**, *151*, No. 104382.
(31) Lin, J.; Zheng, S. Y.; Xiao, R.; Yin, J.; Wu, Z. L.; Zheng, Q.; Qian, J. Constitutive Behaviors of Tough Physical Hydrogels with Dynamic Metal-Coordinated Bonds. *J. Mech. Phys. Solids* **2020**, *139*, No. 103935.
(32) Wang, X.; Hong, W. Pseudo-Elasticity of a Double Network Gel. *Soft Matter* **2011**, *7*, 8576−8581.
(33) Zhao, X. A Theory for Large Deformation and Damage of Interpenetrating Polymer Networks. *J. Mech. Phys. Solids* **2012**, *60*, 319−332.
(34) Mao, Y.; Lin, S.; Zhao, X.; Anand, L. A Large Deformation Viscoelastic Model for Double-Network Hydrogels. *J. Mech. Phys. Solids* **2017**, *100*, 103−130.
(35) Lu, T.; Wang, J.; Yang, R.; Wang, T. J. A Constitutive Model for Soft Materials Incorporating Viscoelasticity and Mullins Effect. *J. Appl. Mech.* **2017**, *84*, No. 021010.
(36) Khiêm, V. N.; Mai, T. T.; Urayama, K.; Gong, J. P.; Itskov, M. A Multiaxial Theory of Double Network Hydrogels. *Macromolecules* **2019**, *52*, 5937−5947.
(37) Ma, J.; Yin, D.; Sheng, Z.; Cheng, J.; Jia, Z.; Li, T.; Qu, S. Delayed Tensile Instabilities of Hydrogels. *J. Mech. Phys. Solids* **2022**, *168*, No. 105052.
(38) Liu, Y.; Zhang, H.; Zheng, Y. A Micromechanically Based Constitutive Model for the Inelastic and Swelling Behaviors in Double Network Hydrogels. *J. Appl. Mech.* **2016**, *83*, No. 021008.
(39) Brown, H. R. A Model of the Fracture of Double Network Gels. *Macromolecules* **2007**, *40*, 3815−3818.
(40) Jia, Y.; Zhou, Z.; Jiang, H.; Liu, Z. Characterization of Fracture Toughness and Damage Zone of Double Network Hydrogels. *J. Mech. Phys. Solids* **2022**, *169*, No. 105090.
(41) Jia, Z.; Nguyen, T. D. A Micromechanical Model for the Growth of Collagenous Tissues under Mechanics-Mediated Collagen Deposition and Degradation. *J. Mech. Behav. Biomed. Mater.* **2019**, *98*, 96−107.
(42) Liu, C.; Du, Y.; Li, K.; Zhang, Y.; Han, Z.; Zhang, Y.; Qu, S.; Lü, C. Geometrical Incompatibility Guides Pattern Selection in Growing Bilayer Tubes. *J. Mech. Phys. Solids* **2022**, *169*, No. 105087.
(43) Fan, Q.; Chen, B. Constitutive Model for the Growth of a Gel Network Regulated by Its Microscopic Mechanics toward a Homeostatic State. *J. Mech. Phys. Solids* **2019**, *130*, 181−194.
(44) Zhang, H.; Hu, Y. A Statistical-Chain-Based Theory for Dynamic Living Polymeric Gels with Concurrent Diffusion, Chain Remodeling Reactions and Deformation. *J. Mech. Phys. Solids* **2023**, *172*, No. 105155.
(45) Marckmann, G.; Verron, E.; Gornet, L.; Chagnon, G.; Charrier, P.; Fort, P. A Theory of Network Alteration for the Mullins Effect. *J. Mech. Phys. Solids* **2002**, *50*, 2011−2028.
(46) Chanda, M. *Introduction To Polymer Science and Chemistry*; CRC Press, 2006.
(47) Wang, Y.; Nian, G.; Kim, J.; Suo, Z. Polyacrylamide Hydrogels. VI. Synthesis-Property Relation. *J. Mech. Phys. Solids* **2023**, *170*, No. 105099.
(48) Pan, Y.; Suo, Z.; Lu, T. A Thermodynamic Model of Phase Transition of Poly(N-Isopropylacrylamide) Hydrogels in Ionic Solutions. *Int. J. Solids Struct.* **2022**, *257*, No. 111434.
(49) Zhong, D.; Xiang, Y.; Yin, T.; Yu, H.; Qu, S.; Yang, W. A Physically-Based Damage Model for Soft Elastomeric Materials with Anisotropic Mullins Effect. *Int. J. Solids Struct.* **2019**, *176-177*, 121−134.

https://doi.org/10.1021/acs.macromol.3c00837
Macromolecules XXXX, XXX, XXX−XXX